molecular pharmaceutics

Article

pubs.acs.org/molecularpharmaceutics

Sustained Expression of the RON Receptor Tyrosine Kinase by Pancreatic Cancer Stem Cells as a Potential Targeting Moiety for Antibody-Directed Chemotherapeutics

Snehal S. Padhye,[†,‡] Sunny Guin,[†,‡] Hang-Ping Yao,[§] Yong-Qing Zhou,[§] Ruiwen Zhang,[†,∥] and Ming-Hai Wang*[,†,‡]

[†]Cancer Biology Center and [‡]Department of Biomedical Sciences, School of Pharmacy, Texas Tech University Health Sciences Center, Amarillo, Texas 79106, United States

[§]National Key Laboratory for Diagnosis and Treatment of Infectious Diseases and Department of Neurosurgery, First Affiliated Hospital, Zhejiang University School of Medicine, Hangzhou, Zhejiang 310003, P. R. China

[∥]Department of Pharmaceutical Sciences, School of Pharmacy, Texas Tech University Health Sciences Center, Amarillo, Texas 79106, United States

ABSTRACT: Cancer stem cells (CSCs) contribute to pancreatic cancer tumorigenesis through tumor initiation, drug resistance, and metastasis. Currently, therapeutics targeting pancreatic CSCs are under intensive investigation. This study tested a novel strategy that utilizes the RON receptor as a drug delivery moiety for increased therapeutic activity against pancreatic CSCs. $CD24^+CD44^+ESA^+$ triple-positive pancreatic CSCs ($CSCs^{+24/44/ESA}$) were obtained from spheroids of pancreatic L3.6pl cancer cells by sequential magnetic cell sorting methods. These cells displayed a spherical growth pattern, expressed the unique self-renewal marker Bmi-1, redifferentiated into an epithelial phenotype, acquired an epithelial to mesenchymal phenotype, and caused tumor formation in animal models. Among several receptor tyrosine kinases examined, RON was highly expressed and sustained by $CSCs^{+24/44/ESA}$. This feature provided the cellular basis for validating the therapeutic effectiveness of anti-RON antibody Zt/c9-directing doxorubicin-immunoliposomes (Zt/c9-Dox-IL). Zt/c9-Dox-IL specifically interacted with $CSCs^{+24/44/ESA}$ and rapidly caused RON internalization, which led to the uptake of liposome-coated Dox. Moreover, Zt/c9-Dox-IL was effective in reducing viability of L3.6pl cells and $CSCs^{+24/44/ESA}$. The IC_{50} values between free Dox ($62.0 \pm 3.1\ \mu M$) and Zt/c9-Dox-IL ($95.0 \pm 6.1\ \mu M$) treated $CSCs^{+24/44/ESA}$ were at relatively comparable levels. In addition, Zt/c9-Dox-IL in combination with small molecule inhibitors lapatinib, sunitinib, or dasatinib further reduced the viability of $CSCs^{+24/44/ESA}$. In conclusion, RON expression by $CSCs^{+24/44/ESA}$ is a suitable molecule for the targeted delivery of chemoagents. The anti-RON antibody-directed delivery of chemotherapeutics is effective in reducing viability of pancreatic CSCs.

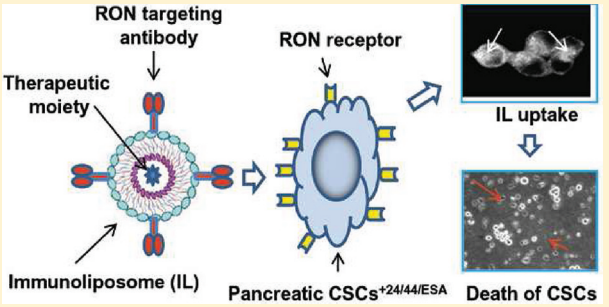

KEYWORDS: *pancreatic cancer stem cell, receptor tyrosine kinase, immunoliposome, drug delivery, targeted therapy*

INTRODUCTION

Cancer-initiating cells, also known as cancer stem cells (CSCs), have been studied in various epithelial tumors, including pancreatic ductal adenocarcinoma (PDAC).[1−3] PDAC is a malignant disease developed through transformation of normal pancreatic cells into precursor pancreatic intraepithelial neoplastic cells.[4] Clinically, early metastasis and acquired chemoresistance are the major pathogenic features of PDAC.[4] Currently, gemcitabine-based chemotherapy is the mainstay, but with limited benefits.[4−6] Small molecule inhibitor erlotinib that targets EGFR has recently been used in combination with gemcitabine to treat PDAC.[7] Again, this therapy exerts little impact on the course of this aggressive cancer.[7] Increasing evidence indicates that the malignancy of PDAC is sustained by CSCs.[2,3,8] CSCs from PDAC are highly tumorigenic and possess the ability to both self-renew and to produce differentiated progeny.[9,10] Acquired PDAC chemoresistance also has been attributed to CSCs.[10,11] An analysis of cellular markers has shown that pancreatic CSCs simultaneously express CD44, CD24, and ESA.[9] A distinct population of CD133 positive pancreatic CSCs also has been shown to determine tumor growth and metastatic activity.[10] In addition, aldehyde dehydrogenase (ALDH)-1α and transcription factor Bmi-1 have been used to validate pancreatic CSCs.[9,10] Recently, experimental therapies using therapeutic antibodies and small molecule inhibitors have been applied to target pancreatic CSCs.[11,12] Results from these preclinical studies show that these agents are effective in eliminating pancreatic CSCs,

Received: April 13, 2011
Revised: October 12, 2011
Accepted: October 20, 2011
Published: October 20, 2011

resulting in long-term disease control in animal models of human PDAC.[11,12]

Altered expression and activation of receptor tyrosine kinases (RTKs) including the epidermal growth factor (EGFR), MET, vascular endothelial growth factor (VEGFR), and RON are commonly observed in epithelial cancers such as PDAC.[4,13−16] The finding that self-renewal in CSCs might be governed by signaling of the EFGR family strongly suggests that RTKs play a pivotal role in CSC pathogenesis.[17,18] Thus, RTK targeting by therapeutic antibodies or SMIs to eliminate CSCs is a logical approach. Another approach is to target RTKs for intracellular delivery of cytotoxic therapeutics to kill drug resistant cancer cells, including CSCs. In this sense, targeted delivery of therapeutic agents through lipid carrier systems such as antibody-directed immunoliposomes (ILs) has attracted particular interest.[19] Recent advances in liposome (LS) technology have yielded "sterically stabilized" or "stealth" LS's with prolonged circulation time and enhanced tumor extravasation.[19] The use of antibodies specific to RTKs in combination with LS technology has provided a platform to improve the therapeutic efficacy of chemoagents.[20,21] Studies using both *in vitro* and *in vivo* models have shown that, by targeting cancer cells overexpressing EGFR or HER2, cetuximab or trastuzumab-directed drug delivery significantly enhances the efficacies of multiple chemoagents against various types of cancer cells.[20,21] Clearly, antibody-directed IL therapy should have potential for targeting distinct tumor populations such as CSCs.

Activation and overexpression of RON contribute to PDAC pathogenesis.[16,22−24] We and others have previously demonstrated that the RON aberration plays a pathogenic role in PDAC.[16,22−28] RON belongs to the MET pro-oncogene family[24] and is mainly expressed in cells of epithelial origin.[16] Immunohistochemical analysis has discovered that RON is overexpressed in more than 30% to 80% of primary and metastatic PDAC samples.[16,22,23] Overexpression often results in RON constitutive phosphorylation, leading to activation of multiple signaling pathways such as MAP kinase and PI-3 kinase cascades.[29] These pathways are essential for PDAC cell migration and matrix invasion.[25,26] Moreover, RON activation regulates VEGF production by several PDAC cell lines.[25] Silencing RON expression promotes PDAC cell apoptotic death and increases gemcitabine sensitivity in cultured pancreatic cancer cells.[25,26] Significantly, the human neutralizing antibody specific to RON shows therapeutic effects on pancreatic xenograft tumor models.[28] Clearly, these studies demonstrate that altered RON expression contributes to PDAC pathogenesis and that targeting RON may have therapeutic significance in clinical applications.

The goal of this study is to determine if RON expressed by pancreatic CSCs is a potential moiety for delivery of chemoagents for enhanced therapeutic activity. Our objective is to demonstrate an important proof-of-principle for an RTK-mediated targeting strategy for eliminating CSCs of PDAC. Using human PDAC L3.6pl cells as the model, $CD24^+CD44^+ESA^+$ pancreatic CSCs were isolated and characterized through various biochemical and biological methods. Among several RTKs analyzed, RON expression was found to be sustained by $CD24^+CD44^+ESA^+$ pancreatic CSCs, which provides the cellular basis for antibody-directed drug delivery. The binding of anti-RON antibody-directed ILs to CSCs causes RON internalization, which enables uptake of the liposomal doxorubicin (Dox). The use of Dox for the current study is to determine if anti-RON-directed IL approach is suitable for the targeted delivery of chemoagents. The IL-mediated drug uptake also resulted in the reduction of CSC viability as compared to nonspecific liposomal Dox-delivery. Thus, the RON receptor expressed by pancreatic CSCs is a suitable targeting moiety for an increased uptake of chemotherapeutic agents.

MATERIALS AND METHODS

Cell Lines, Antibodies, Reagents, and Drugs. The human pancreatic cancer cell line L3.6pl was kindly provided by Dr. G. E. Gallick (University of Texas M.D. Anderson Cancer Center, Houston, TX).[29] Panc-1 cells were from ATCC (Manassas, VA). Human mature macrophage-stimulating protein (MSP) was purified from human plasma by an anti-MSP antibody affinity column followed by high-performance liquid chromatography as previously described.[30] Mouse monoclonal antibody (mAb) Zt/g4 to human RON was used as previously described.[31] Anti-RON mAb Zt/c9 was produced by standard hybridoma methods as previously described.[31] Zt/c9 and Zt/g4 are highly specific and sensitive to human RON and recognize different epitopes in the RON extracellular domain.[31,32] The rabbit IgG antibody (R5029) specific to human RON C-terminal peptide was used as previously described.[31] Rat anti-MET and EGFR IgG antibodies were from eBiosciences (San Diego, CA) and Abcam (Cambridge, MA), respectively. Mouse mAb to VEGFR was from BD Biosciences (San Jose, CA). Mouse mAbs specific to phosphotyrosine (clone PY100), Erk1/2, and AKT were from Cell Signaling Technology, Inc. (Danvers, MA). Rabbit IgG antibodies to transcription factor Bmi-1 and ALDH-1α were from Santa Cruz Biotechnology, Inc. (Santa Cruz, CA). Mouse mAbs to CD24 and CD44 were from BD Biosciences (San Jose, CA), and mouse mAb to human ESA was from eBiosicences (San Diego, CA). Normal mouse IgG and goat antimouse IgG labeled with fluorescein isothiocyanate (FITC) were from Jackson Immunoresearch Lab (West Grove, PA). Small molecule inhibitors (SMIs) including lapatinib, sunitinib, and dasatinib were from LC Laboratories (Woburn, MA). Gemcitabine, methotrexate, and Dox were from Alexis Biochemicals (San Diego, CA). PEGylated-liposomal Dox (PLD) was from Ortho Biotech Products LP (Horsham, PA) and served as the control in various experiments.

Chemicals, Lipids, and IL Preparation. Chemicals and phospholipids (PPL) including cholesterol, hydrogenated soya phosphatidylcholine, and rhodamine phosphatidyl-ethanolamine (RD-PE) were from Avanti Polar Lipids (Birmingham, AL). LS's were prepared by the hydration of thin lipid film and adjusted to the size of 105 ± 10 nM by size-extrusion methods as previously described.[33] Dox loaded into LS's (LS-Dox) was performed using ammonium sulfate exchange methods.[33] The incorporation of fluorescence dye RD into LS's (LS-RD) was carried out using RD-PE as previously described.[33] The incorporation of anti-RON mAb Zt/c9 or normal mouse IgG into LS-Dox to form ILs (Zt/c9-Dox-IL or NIg-Dox-IL) was conducted by the postinsertion technique.[34] Briefly, Zt/c9 and control IgG were first thiolated using Traut's reagents and then conjugated with micelles prepared from $mPEG_{2000}$DSPE:Mal-PEG_{2000}DSPE (4:1 molar ratio) as described previously.[34] The conjugation efficacy for both Zt/c9 and control IgG was at 70%. The amount of IgG incorporation on ILs was determined by 10% sodium dodecyl sulfate−polyacrylamide gel electrophoresis (SDS-PAGE) analysis using IgG standards followed by densitometry analysis.[33] The amounts of Zt/c9 and normal

mouse IgG inserted on ILs were 45 ± 4 μg and 48 ± 6 μg of proteins per mg of PPL per 200 ± 30 μg of Dox, respectively. The rate of Dox leakage between LS's and ILs was tested at 37 °C. Differences between the two preparations were not observed.

Spheroid Formation and Isolation of Pancreatic CSCs from L3.6pl Cells. We used a two-step approach to isolate $CD24^+CD44^+ESA^+$ triple-positive pancreatic CSCs. The first step is to generate spheroids as previously described.[10] Single L3.6pl cells were cultured in ultralow adhesion plates in the CSC media (MEM/F12 containing B27 supplement, 10 ng/mL bFGF, and 20 ng/mL EGF). At day 60, the generated spheroid cells were used to isolate triple positive cells expressing $CD44^+$, $CD24^+$, and ESA^+ (designated as $CSCs^{+24/44/ESA}$) by the magnetic cell sorting method that sequentially isolates CD24, CD44, and ESA triple positive cells using individual antibodies. Cell surface and intracellular markers of $CSCs^{+24/44/ESA}$ were determined by various biochemical and biological methods.

Western Blotting, Immunoprecipitation, and Protein Phosphorylation Assays. Western blot analysis was performed as previously described.[16] Rabbit IgG antibody (R5029) was used to detect RON followed by enhanced chemiluminescent reagents (Thermo Scientific, Meridian, IL). To determine RON phosphorylation, cells were stimulated with MSP or Zt/c9 for 15 min at 37 °C, lysed in lysis buffer, and then immunoprecipitated with anti-RON mAb Zt/g4. Phosphorylated RON was detected by Western blotting using mAb PY100. Phosphorylation of Erk1/2, AKT, and other proteins was determined by Western blotting using individual antibodies as previously described.[16]

Immunofluorescence Analysis of Zt/c9 Binding and RON Internalization in L3.6pl Cells and CSCs. Cell surface-binding activities of Zt/c9 and other mAbs were determined as previously described.[33] L3.6pl cells at 1×10^5 cells/sample were incubated with 2 nM of individual mAbs at 4 °C for 45 min followed by the addition of antimouse IgG coupled with FITC. Normal mouse IgG was used as the control. To determine if Zt/c9 competes with MSP for RON binding, cells were treated with 2 nM of Zt/c9 in the presence or absence of increased amounts of MSP. To determine if Zt/c9 induces RON internalization, cells were first incubated at 37 or 4 °C with 1 μg of Zt/c9 for 60 min and then washed with an acidic buffer (150 mM NaCl, pH 2.5) to eliminate antibodies bound on the cell surface.[33] Cells without acidic wash served as the control. In certain experiments, cells were treated with 10 μg/mL of endocytic inhibitor cytochalasin B (*Cc*-B) to verify if the inhibition of receptor internalization occurs.[33] Cell surface fluorescence intensities were measured and determined by BD FACScan as described previously.[33]

Methods for Measuring Cellular Uptakes of Zt/c9-RD-IL. Three methods were used to determine cellular uptake of Zt/c9-directed IL. The first is a confocal microscope-based method, in which RD is used as the indicator of cellular uptake.[33] L3.6pl cells or $CSCs^{+24/44/ESA}$ were treated at 37 °C with Zt/c9-RD-IL in the presence or absence of excessive free Zt/c9 (2 μg of IgG per sample) for 60 min. Cells treated with NIg-RD-IL served as the control. After incubation, cells were washed with PBS, fixed with 4% paraformaldehyde solution, and then observed under the Olympus DSU confocal microscope. The second method uses the uptake of PPL by cells as the indicator.[33] In this assay, the fluorescence intensities of RD were quantitatively measured and then converted into the amounts of PPL incorporated into Zt/c9-RD-IL.[33] Briefly, cells were incubated with various amounts of Zt/c9-RD-IL or NIg-RD-IL at 4 or 37 °C for 60 min and then washed with PBS. The fluorescence intensities from cell lysates were measured by a Bio-TeK fluorescence microplate reader (excitation at 557 nm and emission at 571 nm, Winooski, VT). The uptake was calculated and converted to the amounts of PPL associated with cells.[33] The third method directly measured the amounts of cell-associated Dox after cells were incubated at 37 °C for 60 min with Zt/c9-Dox-IL as previously described.[33] NIg-Dox-IL was used as the control. After extensive washing, cells were lysed. The fluorescence emission of Dox in cell lysates was measured at 592 nm using the Bio-Tek fluorescence microplate reader.

MTS Assays for Cell Viability. The sensitivity of L3.6pl cells and $CSCs^{+24/44/ESA}$ to individual chemoagents, SMIs, and Zt/c9-directed ILs was determined using the MTS assay as previously described.[33] Cells (1×10^4 cells per well in triplicate in a 96-well plate) were treated with various amounts of chemoagents, Zt/c9-Dox-IL, or SMIs. For measuring IC_{50} of free chemoagents and SMIs, cells were treated with drugs for 72 h. For measuring IC_{50} of PLD, Zt/c9-Dox-IL, and NIg-Dox-IL, cells were treated only for 60 min followed by washing. The 60 min treatment is necessary to avoid nonspecific interaction of LS's with the cell membrane, leading to an increase in drug uptake. In all cases, cell viability was determined at 72 h by measuring the remaining viable cells. Percentages of viable cells were defined as the treatment group divided by control group, multiplied by 100%. Growth inhibition caused by SMIs was determined by comparing treatment groups with the control cells defined as 100% of growth to reach the percentage of growth inhibition. IC_{50} values from experimental and control groups were calculated as previously described.[33]

CSCs *in Vivo* Tumorigenic Assay. Isolated triple positive $CSCs^{+24/44/ESA}$ (500 cells in 50 μL PBS per site) were subcutaneously injected into the hindflank region of athymic nude mice (six mice per group). L3.6pl cells (10,000 cells per injection) were used as the control. Mice were monitored for 40 days for tumor growth as previously described.[10]

Statistical Analysis. Experiments were performed at least two or three times with samples tested in triplicate. Results were expressed as mean ± SEM All statistical analyses were conducted using Prism 3.0 statistical software (GraphPad Software Inc., San Diego, CA). Data were analyzed either by Student's *t* test or by one-way or two-way analysis of variance (ANOVA) in conjunction with Tukey's posthoc test to determine differences among individual groups. Differences were considered statistically significant at $p < 0.05$.

RESULTS

$CD24^+CD44^+ESA^+$ Spheroid Cells Derived from Pancreatic Cancer L3.6pl Cells Display the Stem Cell Phenotype. Isolation of $CSCs^{+24/44/ESA}$ was performed by a two-step method using L3.6pl cells which are known to generate CSCs.[10,35] $CSCs^{+24/44/ESA}$ grew as spheres when they were cultured in CSC media (Figure 1A). Flow cytometric analysis revealed that more than 97% of isolated cells were triple positive for CSC markers of $CD24^+$, $CD44^+$, and ESA^+ (Figure 1B). Interestingly, CD133 expression was not increased and barely detected in $CSCs^{+24/44/ESA}$ (data not shown). Expression of transcription factor Bmi-1,[9,10] a marker for self-renewal, was detected in $CSCs^{+24/44/ESA}$ but not in parental L3.6pl cells. Moreover, increased ALDH-1α expression,[9,10] known as the functional marker for CSCs and progenitor cells,

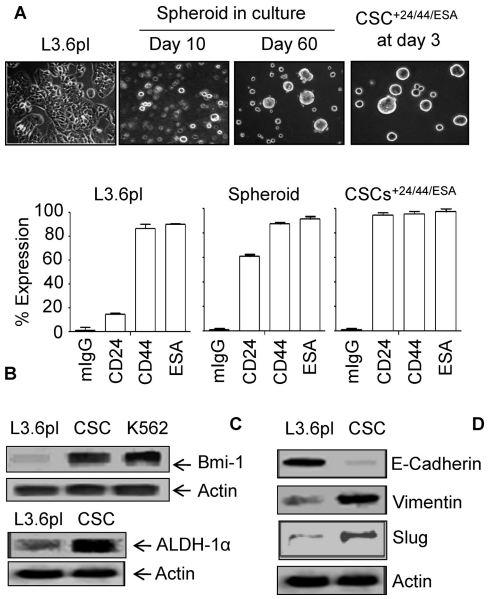

Figure 1. Phenotypes of pancreatic CSCs$^{+24/44/ESA}$ isolated from L3.6pl cells. (A) L3.6pl cells showed typical epithelial morphologies in MEM containing 10% FBS. Spheroid cells were generated by culturing cells in ultralow adhesion plates in CSCs media. At day 60, CSCs$^{+24/44/ESA}$ were isolated from spheroid cells by the magnetic cell sorting method that sequentially isolates CD24, CD44, and ESA triple positive cells using individual antibodies. The image of CSC$^{+24/44/ESA}$ was taken 48 h after isolation. (B) L3.6pl, spheroid, and CSCs$^{+24/44/ESA}$ (0.5×10^5 cells per sample) were incubated at 4 °C with individual antibodies specific to CD24, CD44, ESA, and CD133, followed by antimouse IgG coupled with FITC. Normal mouse IgG was used as the control. The percentages of $CD24^+CD44^+ESA^+$ triple-positive cells were more than 97%. The fluorescence intensity was determined as previously described.[31] (C) Cell lysates (50 μg per sample) from adherent L3.6pl and cultured CSCs$^{+24/44/ESA}$ were subjected to Western blot analysis to determine Bmi-1 and ALDH-1α expression. Cellular proteins from K562 cells were used as the positive control for Bmi-1. β-actin was used as the sample loading control. (D) Western blot detection of E-cadherin, vimentin, and slug in cellular proteins from CSCs$^{+24/44/ESA}$ was performed using individual specific antibodies as described in C. β-actin was used as the sample loading control. Data shown here are from one of three experiments with similar results.

was detected in CSCs$^{+24/44/ESA}$ (Figure 1C). The analysis of E-cadherin and vimentin by Western blotting confirmed that CSCs$^{+24/44/ESA}$ display a phenotype of the epithelial to mesenchymal transition (EMT), which is characterized by a diminished epithelial appearance and gain of mesenchymal phenotype (Figure 1D).[36] Expression of the transcription repressor Slug, which regulates EMT,[37] also was increased in CSCs$^{+24/44/ESA}$. These observations were consistent with CSCs isolated from clinical PDAC samples as reported previously.[9]

A functional study showed that, when CSCs$^{+24/44/ESA}$ were reintroduced into FBS containing culture media, a polarized epithelial morphology reappeared with formation of tight junctions (Figure 2A). Such an appearance was indistinguishable from morphologies of parental L3.6pl cells. The fluorescence analysis of CD24, CD44, and ESA in redifferentiated cells 15 days after regular culture revealed that percentages of $CD24^+$ cells were dramatically reduced. A reduction of $CD44^+$ and ESA^+ cells also was observed (Figure 2B). An analysis of cellular proteins confirmed that epithelial marker E-cadherin reappeared in the differentiated cells, which was accompanied by diminished slug expression (Figure 2C).

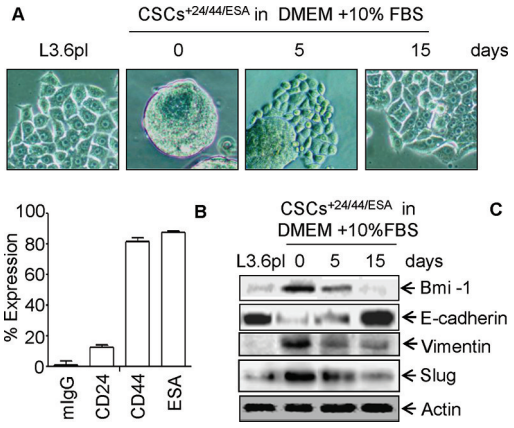

Figure 2. Differentiation of CSCs$^{+24/44/ESA}$ in FBS containing media. (A) Spheroids of CSCs$^{+24/44/ESA}$ were cultured in MEM containing 10% FBS and epithelial morphologies reappeared. L3.6pl cells were used as the control. (B) Differentiated CSCs$^{+24/44/ESA}$ were subjected to immunofluorescence analysis as described in Figure 1B. Levels of CD24, CD44, and ESA expression were observed. (C) Diminished Bmi-1 and increased E-cadherin expression in differentiated CSCs$^{+24/44/ESA}$ was determined by Western blot analysis using specific antibodies. L3.6pl cells and CSCs$^{+24/44/ESA}$ were used as the control. Data shown here are from one of three experiments with similar results.

These phenotypic changes also were associated with a diminished expression of Bmi-1 in the redifferentiated cells (Figure 2C). These results suggest that CSCs$^{+24/44/ESA}$ have the ability to differentiate into epithelial cell phenotype. Finally, *in vivo* studies confirmed that CSCs$^{+24/44/ESA}$ caused tumor growth when cells (500 cells per site) were injected into athymic nude mice (five positive results from six injected mice). In contrast, an injection of L3.6pl cells at 10 000 cells per site did not form tumors in control mice (six negative results from six injected mice). Thus, results in Figures 1 and 2 demonstrate that CSCs$^{+24/44/ESA}$ derived from L3.6pl cells display stem cell-like phenotype.

CSCs$^{+24/44/ESA}$ Are Less Sensitive to Therapeutic Activities of Chemoagents and SMIs. Drug-sensitivity profiles of CSCs$^{+24/44/ESA}$ toward chemoagents gemcitabine, methotrexate, and Dox are shown in Table 1. Cells were treated with individual drugs for 72 h followed by the MTS assay. L3.6pl cells were highly sensitive to drug treatment with reduced cell viability. The IC_{50} value was 6.0 nM for gemcitabine, 9.0 nM for methotrexate, and 90.0 nM for Dox. In contrast, the IC_{50} values from CSCs$^{+24/44/ESA}$ treated with the same drugs increased greatly, ranging from 94.0 nM for gemcitabine, 210.0 nM for methotrexate, and 850.0 nM for Dox. These results suggest the extremely low sensitivities of CSCs$^{+24/44/ESA}$ toward three chemotherapeutic agents.

We also tested the growth-inhibitory effect of lapatinib, dasatinib, and sunitinib on CSCs$^{+24/44/ESA}$ (Table 1). Again, L3.6pl cells were sensitive to the inhibitory effect of these SMIs. The IC_{50} value was 2.0 μM for lapatinib, 0.7 μM for dasatinib, and 1.8 μM for sunitinib. In contrast, CSCs$^{+24/44/ESA}$ showed reduced sensitivity to SMIs with the IC_{50} values at 28 μM for lapatinib, 5.0 μM for dasatinib, and 8.7 μM for sunitinib. Regardless of the mechanisms involved in drug sensitivity, results in Table 1 indicate that CSCs$^{+24/44/ESA}$ were insensitive to the chemoagent-induced effect. Their sensitivity toward SMI-induced growth inhibition also was reduced compared to L3.6pl cells.

dx.doi.org/10.1021/mp200193u | *Mol. Pharmaceutics* 2011, 8, 2310–2319

Table 1. Therapeutic Activity of Chemoagents and Small Molecule Inhibitors (SMIs) in the Viability of L3.6pl Cells and CSCs$^{+24/44/ESA}$ [a]

drug	biomolecules affected	effect (IC_{50}, μM) on L3.6pl	effect (IC_{50}, μM) on CSCs$^{+CD24/44/ESA}$	fold increase[b]
		Chemoagents		
gemcitabine	DNA and ribonucleotide reductase	0.006 ± 0.002	0.094 ± 0.008	15.7
methotrexate	metabolic enzymes DHFR, TS, and others	0.009 ± 0.001	0.21 ± 0.12	23.3
doxorubicin	Topoisomerase II and DNA	0.09 ± 0.01	0.85 ± 0.02	9.4
		Targeted SMIs		
lapatinib	EGFR and Her2	2.0 ± 0.08	28.0 ± 1.1	14.0
dasatinib	Bcr/abl, Src, c-Kit, and Eph kinases	0.7 ± 0.1	5.00 ± 0.23	7.2
sunitinib	PDGFr, VEGFR, C-Kit, Ret, and Flt3	1.8 ± 0.024	8.7 ± 0.55	4.8

[a]Cells (1×10^4 cells per well in triplicate in a 96-well plate) were treated for 72 h at 37 °C with various amounts of chemoagents or SMIs. Cell viability was determined by the percentage of remaining viable cells. The cytostatic effect caused by SMIs presented as a percentage of growth inhibition. Results shown here are from one of three experiments with similar results. [b]The fold increase was calculated by values from CSCs$^{+24/44/ESA}$ divided by values from L3.6pl cells.

Sustained RON Expression and Activation in L3.6pl-Derived CSCs$^{+24/44/ESA}$. Altered RTK expression occurs in PDAC and is a potential therapeutic target.[4,7] Using immunofluorescence cell surface analysis, we determined RON, MET, EGFR, and VEGFR expression by CSCs$^{+24/44/ESA}$ (Figure 3A). MET and VEGFR were minimally expressed by L3.6pl cells and CSCs$^{+24/44/ESA}$. EGFR expression was relatively high in L3.6pl cells but moderately reduced in CSCs$^{+24/44/ESA}$. To our surprise, RON expression was sustained in CSCs$^{+24/44/ESA}$, although a moderate reduction was observed compared to levels of RON in L3.6pl cells. Results from Western blotting of MET, VEGFR, and EGFR expression by CSCs$^{+24/44/ESA}$ (data not shown) were consistent with those from immunofluorescence analysis. Only a sustained RON expression was detected in CSCs$^{+24/44/ESA}$ (Figure 3B,a), and its expression levels were consistent with those from flow cytometric analysis.

RON-mediated signaling events were studied by stimulation of CSCs$^{+24/44/ESA}$ with ligand MSP or Zt/c9 (Figure 3B,a). MSP and Zt/c9 strongly induced RON phosphorylation in CSCs$^{+24/44/ESA}$. Stimulation also caused phosphorylation of Erk1/2 and AKT (Figure 3B,b and c). To verify if RON activation exerts any biological effects, RON-mediated proliferation of L3.6pl cells or CSCs$^{+24/44/ESA}$ was determined by using the MTS assay (Figure 3C). MSP slightly increased L3.6pl cell numbers in a time-dependent manner. However, this effect was not observed in CSCs$^{+24/44/ESA}$, indicating the minimal effect of MSP on the growth of CSCs$^{+24/44/ESA}$. We then studied whether RON activation decreases the drug sensitivity of CSCs$^{+24/44/ESA}$. Consistent with results shown in Table 1, CSCs$^{+24/44/ESA}$, in comparison with L3.6pl cells, showed reduced sensitivity to the gemcitabine-induced effect with the IC_{50} value at about 97 nM (Figure 3D). MSP stimulation did not further change the drug sensitivity of CSCs$^{+24/44/ESA}$. Thus, results in Figure 3 indicate that RON is expressed and activated by MSP or Zt/c9. However, such activation was not sufficient to increase proliferation and to decrease the drug sensitivity of CSCs$^{+24/44/ESA}$.

Zt/c9 Effectively Induces RON Internalization and Subsequent Dox-IL Uptake by CSCs$^{+24/44/ESA}$. Sustained RON expression—but not other RTKs—in CSCs$^{+24/44/ESA}$ prompted us to determine if RON is suitable as a targeting moiety for antibody-directed drug delivery. Anti-RON mAb Zt/c9 was selected because of its high specificity and sensitivity to RON and because it does not compete with MSP for receptor

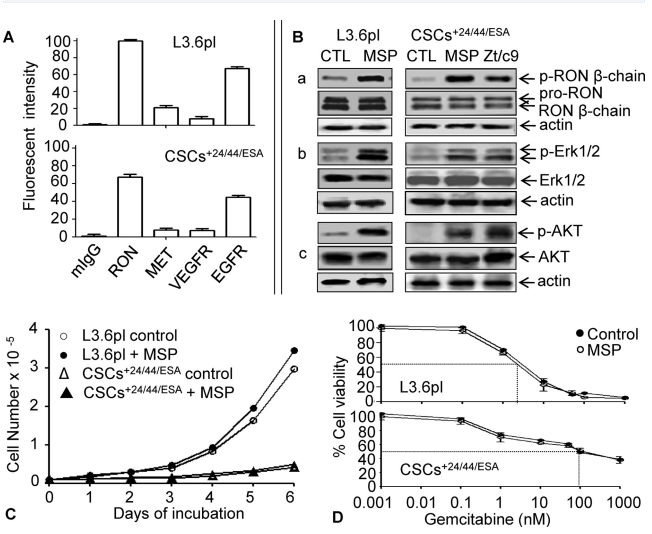

Figure 3. Sustained RON expression, activation, and biological activities in CSCs$^{+24/44/ESA}$. (A) Individual RTK expression by L3.6pl cells or CSCs$^{+24/44/ESA}$ was performed by immunofluorescence analysis as described in Figure 1B. Cells at 0.5×10^5 cells per sample were incubated with individual antibodies followed by FITC-coupled second antibody. Normal mouse IgG was used as the control. The fluorescence intensity was determined as previously described.[31] (B) L3.6pl cells or CSCs$^{+24/44/ESA}$ (1.5×10^6 cells per sample) were stimulated at 37 °C with 2 nM of MSP or Zt/c9 for 15 min. Phosphorylated RON was determined by Western blotting using mAb PY100 after immunoprecipitation of RON with anti-RON mAb Zt/g4 from cell lysates (100 μg per sample). Phosphorylated Erk1/2 and AKT were directly detected from cell lysates by Western blotting using individual antiphospho-antibodies. Membranes were also reprobed with antibodies to RON, Erk1/2, or AKT to verify levels of individual protein expression. Levels of actin were used as the loading control for each protein. MSP-induced cell proliferation was performed by incubating L3.6pl or CSCs$^{+24/44/ESA}$ (1×10^4 cells/well in triplicate) in a 96-well plate with 2 nM of MSP for various days. Unstimulated cells were used as the control. Cell growth was determined by the MTS assay, and cell numbers were obtained as previously described.[31] (D) MSP-regulated drug sensitivity of L3.6pl cells or CSCs$^{+24/44/ESA}$ was determined by incubating cells (0.5×10^5 cells per well in triplicate in a 96-well plate) with or without different amounts of gemcitabine for 60 min followed by washing and medium change. Cell viability was determined by the MTS assay. The % of cell viability was calculated as previously described.[33] Data shown here are from one of three experiments with similar results.

dx.doi.org/10.1021/mp200193u|Mol. Pharmaceutics 2011, 8, 2310–2319

binding (Figure 4A and B). Binding of Zt/c9 to RON on L3.6pl cells also rapidly induced RON internalization, which

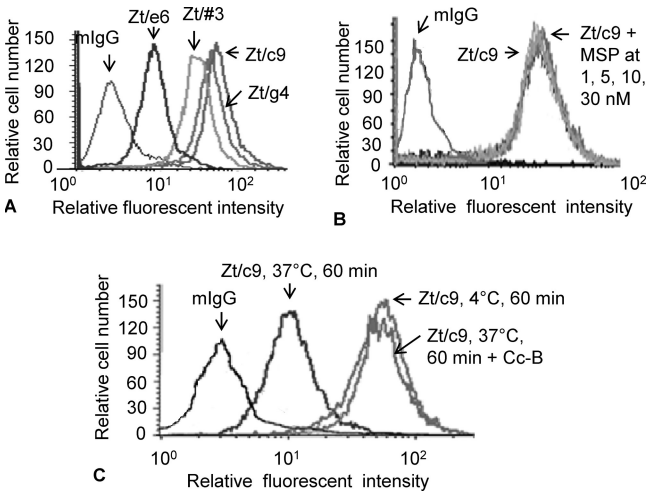

Figure 4. Biochemical features of Zt/c9 in competion with MSP binding and RON internalization. L3.6pl cells (2×10^5 cells per sample) were incubated with 2 nM of Zt/c9 for 45 min. Normal mouse IgG was used as the control. Immunofluorescence was determined as previously described.[31] (A) Binding of Zt/c9 and other anti-RON mAbs to RON was performed at 4 °C by incubating cells with individual mAbs followed by goat-antimouse IgG coupled with FITC. Zt/g4 was used as the positive control. (B) Zt/c9 in competition with MSP in binding to RON was performed by incubating cells at 4 or 37 °C with Zt/c9 with different amounts of MSP for 45 min. Cells incubated with Zt/c9 alone were used as the positive control. (C) Anti-RON mAb-induced RON internalization was determined by incubating cells with Zt/c9 at 37 °C followed by washing with acidic buffer to remove cell surface-bound IgG. Endocytic inhibitor Cc-B (10 μg/mL) was used to inhibit endocytosis. Cells incubated with Zt/c9 at 4 °C were used as the control. The RON receptor remaining on the cell surface was detected by FITC-labeled Zt/g4 as previously described.[27] Data shown here are from one of two experiments with similar results.

was prevented by endocytic inhibitor Cc-B (Figure 4C). To further study Zt/c9-induced RON internalization, we used a confocal microscope to analyze Zt/c9-induced RON internalization. RD-loaded Zt/c9-IL was prepared (Zt/c9-RD-IL) and used as an indication marker. As the control, incubation of CSCs$^{+24/44/ESA}$ with NIg-RD-IL did not show visible fluorescence either on the cell surface or in the cytoplasm (Figure 5A). In contrast, high levels of intracellular RD fluorescence were observed in CSCs$^{+24/44/ESA}$ treated with Zt/c9-RD-IL (Figure 5A). In control L3.6pl cells, cytoplasmic fluorescence also was seen after the addition of Zt/c9-RD-IL, but not NIg-RD-IL.

To study IL uptake in more detail, PPL from Zt/c9-RD-IL was used as the indication marker. L3.6pl cells and CSCs$^{+24/44/ESA}$ were treated with different amounts of Zt/c9-RD-IL or NIg-RD-IL (adjusted to the levels of PPL) for 1 h or 3 h at 37 °C. We observed a marked increase in the amount of PPL associated with CSCs$^{+24/44/ESA}$ treated with Zt/c9-RD-IL (Figure 5B). The increased uptake by CSCs$^{+24/44/ESA}$ was slightly lower than that of control L3.6pl cells treated with Zt/c9-RD-IL. In contrast, no dramatic increase was seen in cells treated with NIg-RD-IL. These results suggest that Zt/c9-RD-IL uptake was increased through a Zt/c9-mediated mechanism.

To verify the above results, levels of Dox associated with CSCs$^{+24/44/ESA}$ after treatment with NIg-Dox-IL or Zt/c9-Dox-IL

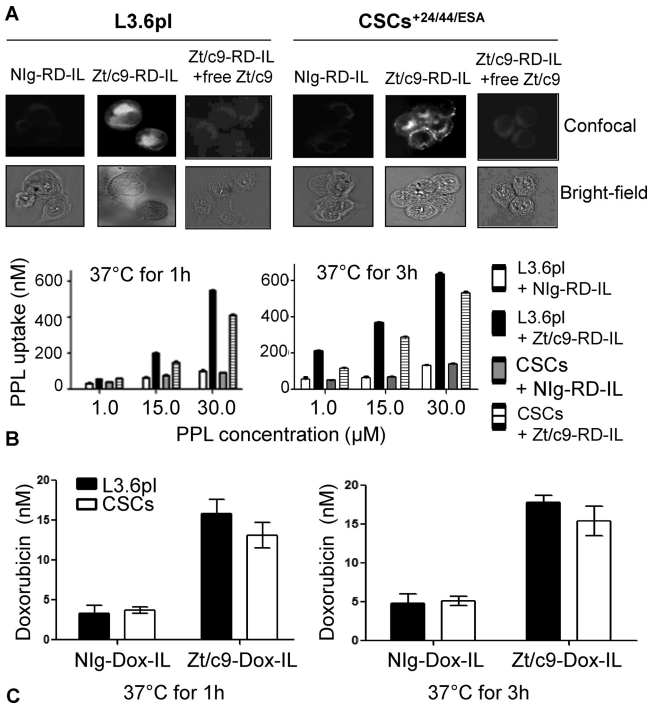

Figure 5. Zt/c9-mediated immunoliposome internalization by CSCs$^{+24/44/ESA}$ and subsequent drug uptake. (A) Confocal analysis of Zt/c9-induced RD-IL internalization: L3.6pl cells or CSCs$^{+24/44/ESA}$ (1×10^4 cells/slide) were treated with Zt/c9-RD-IL (equivalent to 1 μM PPL) at 37 °C for 60 min. Free Zt/c9 (2 μg per sample, a 30-fold increase compared to the amount of the inserted Zt/c9 in RD-IL) was used for competitive inhibition. Cells treated with NIg-RD-IL served as the control. RD was used as the fluorescence indicator. After treatment, cells were washed and fixed with 4% formaldehyde solution. The cell morphology was observed and photographed under bright field. Intracellular fluorescence was determined using the Olympus DSU confocal microscope. (B) Time-dependent internalization of Zt/c9-RD-IL by CSCs$^{+24/44/ESA}$: L3.6pl cells or CSCs$^{+24/44/ESA}$ (2×10^5 cells/sample) were incubated with Zt/c9-RD-IL (equivalent to 1.0, 15.0, and 30.0 μM PPL) at 37 °C for 1 or 3 h followed by the measurement of fluorescence intensities using flow cytometry analysis. Cells treated with NIg-RD-IL served as the control. The amount of RD fluorescence was converted to PPL as previously described.[33] (C) Cells were treated with Zt/c9-Dox-IL (equivalent to 2.0 μM PPL) as described in B. Dox uptake was measured as described in the Materials and Methods section. Data shown here are from one of three experiments with similar results.

were directly measured by fluorescence emission of Dox at 592 nm.[20] Results in Figure 5C show that, after incubation for 1 h or 3 h, the amount of Dox in Zt/c9-IL treated CSCs$^{+24/44/ESA}$ was higher than that of CSCs$^{+24/44/ESA}$ treated with NIg-Dox-IL. Similar results were also observed when L3.6pl cells were used, which showed a relatively higher uptake of Zt/c9-Dox-IL. Thus, as shown by confocal analysis, PPL quantitation, and Dox measurement, Zt/c9 effectively induced RON internalization, which leads to the uptake of Dox by CSCs$^{+24/44/ESA}$.

Zt/c9-Directed Dox-IL Effectively Exerts Therapeutic Activity against CSCs$^{+24/44/ESA}$. The effect of Zt/c9-Dox-IL on the viability of CSCs$^{+24/44/ESA}$ is shown in Table 2. Experiments were performed in which cells were treated for only 60 min with different amounts of free Dox, PLD, NIg-Dox-IL, and Zt/c9-Dox-IL. Such a short period of treatment avoids the increase in drug uptake caused by nonspecific interaction of LS's with the cell membrane. Under such

Table 2. Therapeutic Effect of Zt/c9-Dox-IL *in Vitro* on the Viability of CSCs$^{+CD24/44/ESA}$ [a]

		effect of Dox-containing drugs (IC_{50}, μM) on cell viability				IC_{50} ratio
cell line tested	RON Exp by RT-PCR/WB[b]	free Dox	PLD	NIg-Dox-IL	Zt/c9-Dox-IL	Zt/c9-Dox-IL/free Dox
Panc-1	−/−	11.0 ± 4.0	161.0 ± 23.0	143.0 ± 19.0	149.2 ± 5.9	13.56
L3.6pl	+++/+++	8.0 ± 0.3	103 ± 3.0	99.0 ± 6.0	15.0 ± 3.7	1.88
CSCS$^{+24/44/ESA}$	++/++	62.0 ± 3.1	>300	>300	95.0 ± 6.1	1.53

[a]Panc-1, L3.6pl, and CSCs$^{+24/44/ESA}$ (1×10^4 cells per well) were seeded in a 96-well tissue culture plate in triplicate in DMEM + 10% FBS, MEM + 10% FBS, and serum-free stem cell culture media, respectively, and then treated at 37 °C with different amounts of individual drugs for 60 min followed by washing twice with culture medium. Cells were incubated for additional 72 h followed by the MTS assay to determine cell viability. The IC_{50} values from individual groups were calculated as previously described.[33] Data shown here are from one of two experiments with similar results. [b]RON expression was determined by RT-PCR and Western blot analyses using RON cDNA and cDNA-transfected cells as the control. The levels of mRNA expression and protein expression was determined as −: negative; ++: moderate positive; and +++: strong positive.

conditions, IC_{50} values were higher than those from cells treated for 72 h (Tables 1 and 2).

The requirement of RON expression for drug-reduced cell viability was first examined (Figure 6 and Table 2). Panc-1 cells

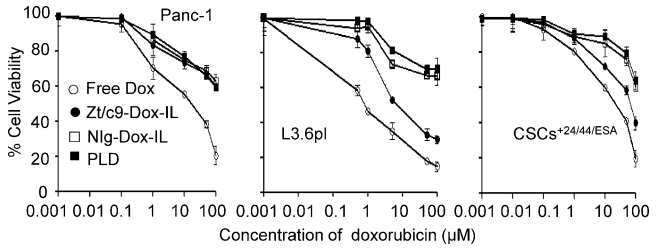

Figure 6. Increased therapeutic effect of Zt/c9-Dox-IL on CSCs$^{+24/44/ESA}$. Cells (1×10^4 cells/well in triplicate in a 96-well plate) were treated for 60 min with various amounts of Zt/c9-Dox-IL. Dox, PLD, and NIg-Dox-IL were used as the controls. To determine if RON is required for Zt/c9-Dox-IL-mediated effect, Panc-1 cells lacking RON expression were used as the control. L3.6pl cells were also used to compare the effectiveness of Zt/c9-Dox-IL in reducing CSCs$^{+24/44/ESA}$ viability. After washing and medium changing, cells were cultured for an additional 72 h, and cell survival was determined by the MTS assay. Data shown here are from one of three experiments with similar results.

lacking RON expression were used as the control. By comparing with L3.6pl cells, Panc-1 cells showed similar sensitivity toward free Dox with IC_{50} at 11.0 μM. However, the amount of Zt/c9-Dox-IL required to achieve IC_{50} values differed from Panc-1 to L3.6pl cells (149.2 μM vs 15.0 μM, respectively). These data suggest that RON expression is required for the observed cell viability reduction. Results from L3.6pl cells treated with Zt/c9-Dox-IL (IC_{50}: 15.0 μM) also revealed that Zt/c9-Dox-IL was effective in reducing L3.6pl cell viability in comparison with the IC_{50} value from cells treated with free Dox (IC_{50}: 8.0 μM; noting the dramatic IC_{50} increase compared to those in Table 1). In contrast, a dramatic increase in IC_{50} values for both PLD (103 μM) and NIg-Dox-IL (99.0 μM) was required for the reduction of L3.6pl cell viability. We should point out that Zt/c9-Dox-IL was not superior to free Dox and that free Dox was more effective in reducing cell viability. Nevertheless, these results suggest that, by binding to RON, Zt/c9 efficiently delivers Dox-IL, causing cell viability reduction after a short treatment of 60 min. The effect of Zt/c9-Dox-IL on the viability of CSCs$^{+24/44/ESA}$ was interesting. Under similar conditions, the IC_{50} value for Zt/c9-Dox-IL was reached at 95.0 μM. This value was relatively comparable to the IC_{50} value of 62.0 μM derived from free Dox treated CSCs$^{+24/44/ESA}$. In contrast, the IC_{50} values from PLD and NIg-Dox-IL treated CSCs$^{+24/44/ESA}$ were not reached even when Dox loaded in NIg-IL was used up to 300 μM (Table 2). Again, we emphasize that, although IC_{50} values increased under such a short period of treatment, the ratios between the IC_{50} from free Dox treated L3.6pl to CSCs$^{+24/44/ESA}$ (ratio: 1.87) and Zt/c9-Dox-IL-treated L3.6pl to CSCs$^{+24/44/ESA}$ (ratio: 1.53) were comparable at a similar range (Table 2). Considering the experimental conditions which yield relatively high IC_{50} values from different groups, the data from cells treated with Zt/c9-Dox-IL suggest that Zt/c9-Dox-IL is effective in reducing the viability of CSCs$^{+24/44/ESA}$.

Zt/c9-Dox-IL in Combination with Small Molecule Inhibitors Displays Increased Therapeutic Activities in CSCs$^{+24/44/ESA}$. Drug-sensitive profiles of CSCs$^{+24/44/ESA}$ from individual chemoagents and SMIs as shown in Tables 1 and 2 and Figure 6 prompted us to determine if Zt/c9-Dox-IL in combination with different SMIs can achieve a maximal effect on the viability of CSCs$^{+24/44/ESA}$. To this end, cells were treated with Zt/c9-Dox-IL, individual SMIs, or their different combinations for 60 min followed by 72 h incubation. As shown in Figure 7, lapatinib and dasatinib at their IC_{50} doses,

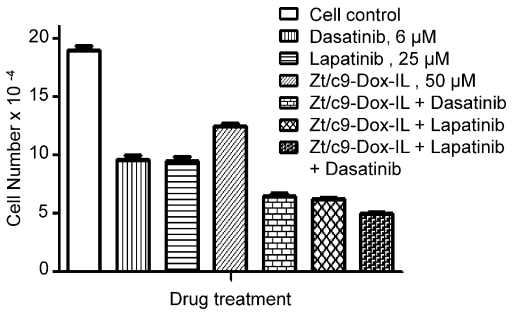

Figure 7. Effect of Zt/c9-Dox-IL in combination with SMIs on reduction of CSCs$^{+24/44/ESA}$ viability. Cells (1×10^4 cells/well in triplicate in a 96-well plate) were treated for 60 min with individual drugs or their different combinations. Untreated cells were used as the control. After washing and medium changing, cells were cultured for additional 72 h followed by the MTS assay. Cell numbers were determined as previously described.[31] Data shown here are from one of three experiments with similar results.

respectively, caused a 50% growth inhibition on CSCs$^{+24/44/ESA}$. Zt/c9-Dox-IL at the IC_{50} dose reduced cell viability by about 50%. The effect was further increased in CSCs$^{+24/44/ESA}$ treated with different drug combinations. The percentages of cell number reduction were at 65.8% for Zt/c9-Dox-IL + dasatinib, 66.7% for Zt/c9-Dox-IL + lapatinib, and 70.4% for Zt/c9-Dox-IL + dasatinib + lapatinib. These results suggest that the

presence of SMIs further increased the effect of Zt/c9-Dox-IL on CSCs$^{+24/44/ESA}$ viability.

DISCUSSION

The findings in this study demonstrate that antibody-directed RON targeting is an effective approach for delivery of chemotherapeutics such as Dox to produce a therapeutic effect on pancreatic CSCs. Using CSCs$^{+24/44/ESA}$ derived from L3.6pl cells as the model, we demonstrated that RTKs are differentially expressed by CSCs$^{+24/44/ESA}$ with variable levels. Among several RTKs analyzed, the RON receptor is highly expressed and sustained by CSCs$^{+24/44/ESA}$. This indicates that RON gene transcription is active in pancreatic CSCs. By binding to an epitope in the RON extracellular domain, Zt/c9 effectively induces RON internalization, which provides a molecular basis for the uptake of ILs loaded with chemoagent. Through such an approach, the increased amounts of Dox uptake by CSCs$^{+24/44/ESA}$ were achieved. We showed that Zt/c9-Dox-IL is effective in reducing viability of L3.6pl cells and CSCs$^{+24/44/ESA}$. The resulting IC_{50} values were reduced compared to those from the control PLD and NIg-Dox-IL. We should point out that Zt/c9-Dox-IL is not superior to free Dox in the *in vitro* cell viability assay. Moreover, we demonstrated that Zt/c9-Dox-IL in combination with SMIs specific to EGFR or other tyrosine kinases increases therapeutic effect on CSCs$^{+24/44/ESA}$. These findings provide an important proof-of-principle for a CSC-targeted, RTK-mediated drug delivery strategy. Thus, Zt/c9-directed delivery of chemotherapeutics may have the potential to be developed into a novel therapeutic with implications for targeting pancreatic CSCs.

Cell surface markers that precisely define pancreatic CSCs are still controversial and are under intensive investigation.[1−3,8] Currently, two sets of accepted cell surface CSC markers, $CD24^+CD44^+ESA^+$ and $CD133^+CXCR4^+$, are established and used to isolate pancreatic CSCs.[9,10] Although showing certain differences in CSC properties, both CSCs$^{+24/44/ESA}$ and CSCs$^{+CD133/CXCR4}$ display very similar functional profiles with various stem cell characteristics, including a tumor-initiating capability, self-renewal activity, ability to produce differentiated progeny, and expression of developmental signaling molecules.[9,10] We believe that different cell surface markers may reflect the distinct population of existing pancreatic CSCs. Using L3.6pl cells as the model followed by two-step (spheroid formation and magnetic sorting) isolation strategy, we isolated CSCs$^{+24/44/ESA}$ for drug delivery analysis. Significantly, $CD133^+$ expression by L3.6pl cells is at very low levels (<1% according to flow cytometry analysis). During the process of spheroid formation, levels of $CD133^+$ spheroid cells remain low (<2%, our unpublished data). An analysis of an isolated CSCs$^{+24/44/ESA}$ population also failed to show an increase in the level of $CD133^+$ cells. These observations indicate that the methods we used seem to not favor the generation of $CD133^+$ CSCs, although some reports have used sorting methods successfully to isolate $CD133^+$ CSCs from L3.6pl cells.[10] Regardless of the methods used to isolate CSCs, results in Figures 1 and 2 confirmed that CSCs$^{+24/44/ESA}$ are capable of forming spheroids when cultured in ultralow adhesion plates in the CSC media and can redifferentiate into epithelial phenotype when recultured in serum-containing media. Intracellular markers, including the transcription factor Bmi-1 and the metabolic enzyme ALDH-1α were highly expressed by CSCs$^{+CD24/44/ESA}$. Moreover, CSCs$^{+24/44/ESA}$ display an EMT-like phenotype with diminished E-cadherin expression and enhanced vimentin expression. The EMT phenotype is known to constitute malignant behavior of CSCs.[36,37] CSCs$^{+24/44/ESA}$ also showed reduced sensitivity in response to cytotoxic and cytostatic activities of chemoagents and SMIs, respectively. Finally, we demonstrated that CSCs$^{+24/44/ESA}$ possess tumor-initiating capability in athymic nude mice. An amount as low as 500 CSCs$^{+24/44/ESA}$ per injection in mouse model is sufficient to cause tumor formation. Thus, CSCs$^{+24/44/ESA}$ belong to a distinct population of pancreatic CSCs.

To validate RTKs as suitable targeting moieties for drug delivery in pancreatic CSCs, we first analyzed several RTK expressions in L3.6pl cells and CSCs$^{+24/44/ESA}$. As shown in Figure 3A, levels of RTKs such as RON, MET, EGFR, and VEGFR varied, indicating that RTKs are differentially expressed in CSCs$^{+24/44/ESA}$. Clearly, it will be important to determine RTK expression patterns in CSCs because the differences among RTK expression could dramatically affect the drug efficacy where specific SMIs or therapeutic targeting antibodies are used. By searching the published literature, we noted that RTK expression profiles of various CSCs were limited. The interesting finding in this study is the high level and sustained expression of RON by CSCs$^{+24/44/ESA}$. This observation is confirmed by cell surface fluorescence analysis and by Western blot analysis. At present, the effect of RON expression on pathogenesis of CSCs$^{+22/44/ESA}$ is still largely unknown. However, our limited studies as shown in Figures 4C and D indicate that MSP does not induce proliferation and change the drug sensitivity in CSCs$^{+24/44/ESA}$, although ligand-induced phosphorylation and activation of RON and downstream signaling molecules such as Erk1/2 and AKT were documented. Treatment of CSCs$^{+24/44/ESA}$ with PHA665752,[38] a MET/RON dual SMI, also failed to inhibit cell growth or cause cell death (our unpublished results), suggesting that RON expression and activation are not sufficient to modulate the CSC phenotype and function. Nevertheless, RON is suitable as a drug delivery carrier moiety due to its efficiency in antibody-induced receptor internalization. With evidence of diminished RON levels on the cell surface followed by Dox uptake (Figures 4 and 5), we demonstrate that the RON receptor is engaged in an active internalization process upon Zt/c9 binding, which ultimately leads to increased uptake of Dox by CSCs$^{+24/44/ESA}$. Inhibition of cellular endocytosis by *Cc*-B completely blocked Zt/c9-induced RON internalization. Furthermore, we demonstrate that the amount of available Dox via antibody-directed uptake is sufficient to reduce the viability of CSCs$^{+24/44/ESA}$ as compared to nonspecific liposomal Dox-delivery. Taken together, results from these studies demonstrate that the sustained RON expression by CSCs$^{+24/44/ESA}$ is a suitable target for antibody-directed Dox-IL delivery for therapeutic purposes.

Elimination of CSCs through pharmaceutical means is currently under intensive investigation.[39] Pancreatic CSCs are highly resistant to conventional chemoagents and often are difficult to destroy.[2,3] Consistent with these observations, we showed that CSCs$^{+24/44/ESA}$ are less sensitive to therapeutic activities mediated by gemcitabine, methotrexate, and Dox. Such a profile indicates that CSCs$^{+24/44/ESA}$ are naturally resistant to chemotherapy. CSCs utilize different mechanisms against the chemo-cytotoxic effect. Recent evidence has shown that certain ATP-binding cassette (ABC) transporters, such as ABCB1 (MDR1), are highly augmented in pancreatic CSCs.[40,41] Inhibition of ABCB1 with the specific blocker verapamil resensitizes the resistant CSCs to gemcitabine,[41] suggesting that blocking or

bypassing ATP-binding transporters could result in increased sensitivity of CSCs toward chemoagents. The advantage of the targeted IL delivery is known to bypass ABC transporters, leading to increased cytotoxic activity.[42] Previous studies have demonstrated that antibody-directed IL is highly effective in the induction of Dox uptake through RON internalization in colon and breast cancer cells.[33] This study provides evidence showing that such an approach is also effective for chemoagent delivery to pancreatic CSCs. As shown in Figure 5, Zt/c9-directed uptake of ILs by $CSCs^{+24/44/ESA}$ was readily detected by confocal observation. The quantitation of cell-associated PPL also indicates the specific uptake of Zt/c9-IL. Measurement of the increased amounts of Dox associated with $CSCs^{+24/44/ESA}$ also has provided indirect evidence of Zt/c9-IL uptake. An analysis of cell viability further demonstrated that Dox uptake is effective in reducing $CSC^{+24/44/ESA}$ viability. As shown in Table 2, the IC_{50} values from Zt/c9-Dox-IL and free-Dox treated $CSCs^{+24/44/ESA}$ are at relatively comparable levels. Specifically, the IC_{50} value from Zt/c9-Dox-IL treated $CSCs^{+24/44/ESA}$ was lower than those from PLD and NIg-Dox-IL treated $CSCs^{+24/44/ESA}$. Clearly, specificity of Zt/c9 to RON provides a platform that promotes the direct interaction of ILs with $CSC^{+24/44/ESA}$, which leads to intracellular Dox uptake and subsequent therapeutic effects.

Molecular-targeted approaches using therapeutic antibodies or SMIs specific to cell surface receptors and intracellular signaling molecules have advanced to various preclinical and clinical stages due to their specificity and effectiveness. Moreover, chemoagents in combination with targeted SMIs also have emerged as a favorable choice for treatment of malignant cancers including PDAC. The rationale for such practices is based mainly on discoveries that various signaling pathways are altered in pancreatic CSCs. To eliminate pancreatic CSCs, various signaling molecules and pathways have been targeted. These include the inhibition of NF-κB pathway by chemopreventive agent sulforaphane,[43] suppression of telomerase activity by imetelstat,[44] inhibition of sonic hedgehog by cyclopamine/CUR199691,[35] blockage of mTOR activity by rapamycin,[35] and activation of cell membrane associated death receptor by a specific antibody.[11] By determining IC_{50} values of L3.6pl cells and $CSCs^{+24/44/ESA}$ in response to lapatinib- and dasatinib-induced growth inhibition, we observed that $CSCs^{+24/44/ESA}$ display variable levels of insensitivity toward these three SMIs. Nevertheless, growth inhibition was still achieved when individual SMIs were used at therapeutic concentrations (Table 1). These results suggest that aberrant expression and activation of signaling molecules such as EGFR and other tyrosine kinases play an important role in regulating tumorigenic phenotypes of $CSCs^{+24/44/ESA}$. Considering these facts, it is conceivable that chemoagents in combination with SMIs could achieve further therapeutic efficacy in reducing the viability of $CSCs^{+24/44/ESA}$. As shown in Figure 7, the reduction in cell numbers mediated by Zt-/c9-Dox-IL was greatly increased by combined treatment with individual SMIs at IC_{50} doses. These results demonstrate that a cooperative effect exists between SMIs and Zt/c9-Dox-IL, which shows increased therapeutic activities against $CSCs^{+24/44/ESA}$.

AUTHOR INFORMATION

Corresponding Author

*Mailing address: Texas Tech University Health Sciences Center, Department of Biomedical Sciences, School of Pharmacy, 1406 S. Coulter Street, Suite 1117, Amarillo, TX 79106. Tel.: 806-356-4750 ext. 231. Fax: 806-356-4034. E-mail: minghai.wang@ttuhsc.edu.

ACKNOWLEDGMENTS

This work was supported in part by National Institutes of Health grant R01 CA91980 and an Amarillo Area Foundation grant to M.H.W. R.W.Z. was supported in part by NIH grants R01CA112029 and R01CA121211. We thank Dr. G.E. Gallick for providing L3.6pl cells. The assistance from Ms. Susan Denney (Office of Sciences, School of Pharmacy at TTUHSC, Amarillo of TX) for professional editing of the manuscript was greatly appreciated.

ABBREVIATIONS USED

ALDH, aldehyde dehydrogenase; ATCC, American Type Culture Collection; bFGF, basic fibroblast growth factor; Cc-B, cytochalasin-B; Dox, doxorubicin; CSC, cancer stem cell; EGFR, epidermal growth factor receptor; EMT, epithelial to mesenchymal transition; ESA, epithelial-specific antigen; FBS, fetal bovine serum; FITC, fluorescein isothiocyanate; IL, immunoliposome; LS, liposome; mAb, monoclonal antibody; MAP, mitogen-activated protein; MSP, macrophage-stimulating protein; MTS, 3-(4,5-dimethyl-thiazole-2-yl)-2,5-diphenyltetrazolium bromide; PDAC, pancreatic ductal adenocarcinoma; PLD, pegylated-liposomal doxorubicin; PPL, phospholipid; RD, rhodamine; RON, recepteur, d'origine nantais; RT-PCR, reverse transcription-polymerase chain reaction; RTK, receptor tyrosine kinase; SMI, small molecular inhibitor; VEGFR, vascular endothelial growth factor receptor

REFERENCES

(1) Rosen, J. M.; Jordan, C. T. The increasing complexity of the cancer stem cell paradigm. *Science* **2009**, *324*, 1670−1673.

(2) Ischenko, I.; Seeliger, H.; Kleespies, A.; Angele, M. K.; Eichhorn, M. E.; Jauch, K. W.; Bruns, C. J. Pancreatic cancer stem cells: new understanding of tumorigenesis, clinical implications. *Langenbecks Arch. Chir.* **2010**, *395*, 1−10.

(3) Lee, C. J.; Dosch, J.; Simeone, D. M. Pancreatic cancer stem cells. *J. Clin. Oncol.* **2008**, *26*, 2806−2812.

(4) Hidalgo, M. Pancreatic cancer. *N. Engl. J. Med.* **2010**, *362*, 1605−1617.

(5) Mihaljevic, A. L.; Michalski, C. W.; Friess, H.; Kleeff, J. Molecular mechanism of pancreatic cancer--understanding proliferation, invasion, and metastasis. *Langenbecks Arch. Chir.* **2010**, *395*, 295−308.

(6) Wang, Z.; Li, Y.; Ahmad, A.; Banerjee, S.; Azmi, A. S.; Kong., D.; Sarkar, F. H. Pancreatic cancer understanding and overcoming chemoresistance. *Nat. Rev. Gastroenterol. Hepatol.* **2011**, *8*, 27−33.

(7) Wong, H. H.; Lemoine, N. R. Pancreatic cancer: molecular pathogenesis and new therapeutic targets. *Nat. Rev. Gastroenterol. Hepatol.* **2009**, *6*, 412−422.

(8) Sergeant, G.; Vankelecom, H.; Gremeaux, L.; Topal, B. Role of cancer stem cells in pancreatic ductal adenocarcinoma. *Nat. Rev. Clin. Oncol.* **2009**, *6*, 580−586.

(9) Li, C.; Heidt, D. G.; Dalerba, P.; Burant, C. F.; Zhang, L.; Adsay, V.; Wicha, M.; Clarke, M. F.; Simeone, D. M. Identification of pancreatic cancer stem cells. *Cancer Res.* **2007**, *67*, 1030−1037.

(10) Hermann, P. C.; Huber, S. L.; Herrler, T.; Aicher, A.; Ellwart, J. W.; Guba, M.; Bruns, C. J.; Heeschen, C. Distinct populations of cancer stem cells determine tumor growth and metastatic activity in human pancreatic cancer. *Cell Stem Cell* **2007**, *1*, 313−323.

(11) Rajeshkumar, N. V.; Rasheed, Z. A.; García-García, E.; López-Ríos, F.; Fujiwara, K.; Matsui, W. H.; Hidalgo, M. A combination of DR5 agonistic monoclonal antibody with gemcitabine targets pancreatic cancer stem cells and results in long-term disease control in human pancreatic cancer model. *Mol. Cancer Ther.* **2010**, *9*, 2582−2592.

(12) Rausch, V.; Liu, L.; Kallifatidis, G.; Baumann, B.; Mattern, J.; Gladkich, J.; Wirth, T.; Schemmer, P.; Büchler, M. W.; Zöller, M.; Salnikov, A. V.; Herr, I. Synergistic activity of sorafenib and

sulforaphane abolishes pancreatic cancer stem cell characteristics. *Cancer Res.* **2010**, *70*, 5004−5013.
(13) Furukawa, T.; Duguid, W. P.; Kobari, M.; Matsuno, S.; Tsao, M. S. Hepatocyte growth factor and Met receptor expression in human pancreatic carcinogenesis. *Am. J. Pathol.* **1995**, *147*, 889−895.
(14) Jin, H.; Yang, R.; Zheng, Z.; Romero, M.; Ross, J.; Bou-Reslan, H.; Carano, R. A.; Kasman, I.; Mai, E.; Young, J.; Zha, J.; Zhang, Z.; Ross, S.; Schwall, R.; Colbern, G.; Merchant, M. MetMAb, the one-armed 5D5 anti-c-Met antibody, inhibits orthotopic pancreatic tumor growth and improves survival. *Cancer Res.* **2008**, *68*, 4360−4368.
(15) Kleespies, A.; Jauch, K. W.; Bruns, C. J. Tyrosine kinase inhibitors and gemcitabine: new treatment options in pancreatic cancer? *Drug Resist. Updates* **2006**, *9*, 1−18.
(16) Wang, M. H.; Lee, W.; Luo, Y. L.; Weis, M. T.; Yao, H. P. Altered expression of the RON receptor tyrosine kinase in various epithelial cancers and its contribution to tumourigenic phenotypes in thyroid cancer cells. *J. Pathol.* **2007**, *213*, 402−411.
(17) Korkaya, H.; Paulson, A.; Iovino, F.; Wicha, M. S. HER2 regulates the mammary stem/progenitor cell population driving tumorigenesis and invasion. *Oncogene* **2008**, *27*, 6120−6130.
(18) Korkaya, H.; Wicha, M. S. HER-2, notch, and breast cancer stem cells: targeting an axis of evil. *Clin. Cancer Res.* **2009**, *15*, 1845−1847.
(19) Hashida, M.; Kawakami, S.; Yamashita, F. Lipid carrier systems for targeted drug and gene delivery. *Chem. Pharm. Bull. (Tokyo)* **2005**, *53*, 871−80.
(20) Mamot, C.; Drummond, D. C.; Noble, C. O.; Kallab, V.; Guo, Z.; Hong, K.; Kirpotin, D. B.; Park, J. W. Epidermal growth factor receptor-targeted immunoliposomes significantly enhance the efficacy of multiple anticancer drugs in vivo. *Cancer Res.* **2005**, *65*, 11631−11638.
(21) Kirpotin, D. B.; Drummond, D. C.; Shao, Y.; Shalaby, M. R.; Hong, K.; Nielsen, U. B.; Marks, J. D.; Benz, C. C.; Park, J. W. Antibody targeting of long-circulating lipidic nanoparticles does not increase tumor localization but does increase internalization in animal models. *Cancer Res.* **2006**, *66*, 6732−6740.
(22) Camp, E. R.; Yang, A.; Gray, M. J.; Fan, F.; Hamilton, S. R.; Evans, D. B.; Hooper, A. T.; Pereira, D. S.; Hicklin, D. J.; Ellis, L. M. Tyrosine kinase receptor RON in human pancreatic cancer: expression, function, and validation as a target. *Cancer* **2007**, *109*, 1030−1039.
(23) Thomas, R. M.; Toney, K.; Fenoglio-Preiser, C.; Revelo-Penafiel, M. P.; Hingorani, S. R.; Tuveson, D. A.; Waltz, S. E.; Lowy, A. M. The RON receptor tyrosine kinase mediates oncogenic phenotypes in pancreatic cancer cells and is increasingly expressed during pancreatic cancer progression. *Cancer Res.* **2007**, *67*, 6075−6082.
(24) Ronsin, C.; Muscatelli, F.; Mattei, M. G.; Breathnach, R. A novel putative receptor protein tyrosine kinase of the met family. *Oncogene* **1993**, *8*, 1195−1202.
(25) Logan-Collins, J.; Thomas, R. M.; Yu, P.; Jaquish, D.; Mose, E.; French, R.; Stuart, W.; McClaine, R.; Aronow, B.; Hoffman, R. M.; Waltz, S. E.; Lowy, A. M. Silencing of RON receptor signaling promotes apoptosis and gemcitabine sensitivity in pancreatic cancers. *Cancer Res.* **2010**, *70*, 1130−1140.
(26) Zhao, S.; Ammanamanchi, S.; Brattain, M.; Cao, L.; Thangasamy, A.; Wang, J.; Freeman, J. W. Smad4-dependent TGF-beta signaling suppresses RON receptor tyrosine kinase-dependent motility and invasion of pancreatic cancer cells. *J. Biol. Chem.* **2008**, *283*, 11293−11301.
(27) Thomas, R. M.; Jaquish, D. V.; French, R. P.; Lowy, A. M. The RON tyrosine kinase receptor regulates vascular endothelial growth factor production in pancreatic cancer cells. *Pancreas* **2010**, *39*, 301−307.
(28) O'Toole, J. M.; Rabenau, K. E.; Burns, K.; Lu, D.; Mangalampalli, V.; Balderes, P.; Covino, N.; Bassi, R.; Prewett, M.; Gottfredsen, K. J.; Thobe, M. N.; Cheng, Y.; Li, Y.; Hicklin, D. J.; Zhu, Z.; Waltz, S. E.; Hayman, M. J.; Ludwig, D. L.; Pereira, D. S. Therapeutic implications of a human neutralizing antibody to the macrophage-stimulating protein receptor tyrosine kinase (RON), a c-MET family member. *Cancer Res.* **2006**, *66*, 9162−9170.
(29) Shah, A. N.; Summy, J. M.; Zhang, J.; Park, S. I.; Parikh, N. U.; Gallick, G. E. Development and characterization of gemcitabine-resistant pancreatic tumor cells. *Ann. Surg. Oncol.* **2007**, *14*, 3629−3637.
(30) Skeel, A.; Yoshimura, T.; Showalter, S. D.; Tanaka, S.; Appella, E.; Leonard, E. J. Macrophage stimulating protein: purification, partial amino acid sequence, and cellular activity. *J. Exp. Med.* **1991**, *173*, 1227−1234.
(31) Yao, H. P.; Luo, Y. L.; Feng, L.; Cheng, L. F.; Lu, Y.; Li, W.; Wang, M. H. Agonistic monoclonal antibodies potentiate tumorigenic and invasive activities of splicing variant of the RON receptor tyrosine kinase. *Cancer Biol. Ther.* **2006**, *5*, 1179−1186.
(32) Li, Z.; Yao, H.; Guin, S.; Padhye, S. S.; Zhou, Y. Q.; Wang, M. H. Monoclonal antibody (mAb)-induced down-regulation of RON receptor tyrosine kinase diminishes tumorigenic activities of colon cancer cells. *Int. J. Oncol.* **2010**, *37*, 473−82.
(33) Guin, S.; Yao, H. P.; Wang, M. H. RON receptor tyrosine kinase as a target for delivery of chemodrugs by antibody directed pathway for cancer cell cytotoxicity. *Mol. Pharmaceutics* **2010**, *7*, 386−397.
(34) Iden, D. L.; Allen, T. M. In vitro and in vivo comparison of immunoliposomes made by conventional coupling techniques with those made by a new post-insertion approach. *Biochim. Biophys. Acta* **2001**, *1513*, 207−216.
(35) Mueller, M. T.; Hermann, P. C.; Witthauer, J.; Rubio-Viqueira, B.; Leicht, S. F.; Huber, S.; Ellwart, J. W.; Mustafa, M.; Bartenstein, P.; D'Haese, J. G.; Schoenberg, M. H.; Berger, F.; Jauch, K. W.; Hidalgo, M.; Heeschen, C. Combined targeted treatment to eliminate tumorigenic cancer stem cells in human pancreatic cancer. *Gastroenterology* **2009**, *137*, 1102−1113.
(36) Mani, S. A.; Guo, W.; Liao, M. J.; Eaton, E. N.; Ayyanan, A.; Zhou, A. Y.; Brooks, M.; Reinhard, F.; Zhang, C. C.; Shipitsin, M.; Campbell, L. L.; Polyak, K.; Brisken, C.; Yang, J.; Weinberg, R. A. The epithelial-mesenchymal transition generates cells with properties of stem cells. *Cell* **2008**, *133*, 704−715.
(37) Christiansen, J. J.; Rajasekaran, A. K. Reassessing epithelial to mesenchymal transition as a prerequisite for carcinoma invasion and metastasis. *Cancer Res.* **2006**, *66*, 8319−8326.
(38) Christensen, J. G.; Schreck, R.; Burrows, J.; Kuruganti, P.; Chan, E.; Le, P.; Chen, J.; Wang, X.; Ruslim, L.; Blake, R.; Lipson, K. E.; Ramphal, J.; Do, S.; Cui, J. J.; Cherrington, J. M.; Mendel, D. B. A selective small molecule inhibitor of c-Met kinase inhibits c-Met-dependent phenotypes in vitro and exhibits cytoreductive antitumor activity in vivo. *Cancer Res.* **2003**, *63*, 7345−7355.
(39) Frank, R. T.; Najbauer, J.; Aboody, K. S. Concise review: stem cells as an emerging platform for antibody therapy of cancer. *Stem Cells* **2010**, *28*, 2084−2087.
(40) Santisteban, M. ABC transporters as molecular effectors of pancreatic oncogenic pathways: the Hedgehog-GLI model. *J. Gastrointest. Cancer* **2010**, *41*, 153−158.
(41) Hong, S. P.; Wen, J.; Bang, S.; Park, S.; Song, S. Y. CD44-positive cells are responsible for gemcitabine resistance in pancreatic cancer cells. *Int. J. Cancer* **2009**, *125*, 2323−2331.
(42) Huwyler, J.; Cerletti, A.; Fricker, G.; Eberle, A. N.; Drewe, J. By-passing of P-glycoprotein using immunoliposomes. *J. Drug Target* **2002**, *10*, s73−79.
(43) Kallifatidis, G.; Rausch, V.; Baumann, B.; Apel, A.; Beckermann, B. M.; Groth, A.; Mattern, J.; Li, Z.; Kolb, A.; Moldenhauer, G.; Altevogt, P.; Wirth, T.; Werner, J.; Schemmer, P.; Büchler, M. W.; Salnikov, A. V.; Herr, I. Sulforaphane targets pancreatic tumour-initiating cells by NF-κB-induced antiapoptotic signalling. *Gut* **2009**, *58*, 949−963.
(44) Joseph, I.; Tressler, R.; Bassett, E.; Harley, C.; Buseman, C. M.; Pattamatta, P.; Wright, W. E.; Shay, J. W.; Go, N. F. The telomerase inhibitor imetelstat depletes cancer stem cells in breast and pancreatic cancer cell lines. *Cancer Res.* **2010**, *70*, 9494−9504.